Available online at http://scik.org
Commun. Math. Biol. Neurosci. 2024, 2024:134
https://doi.org/10.28919/cmbn/8948
ISSN: 2052-2541

MODELING AND PREDICTING THE SPREAD OF DIPHTHERIA IN GUINEA USING DELAYED STOCHASTIC DIFFERENTIAL EQUATIONS

ISSAM SAHIB[1,*], BENYOUNES BETTIOUI[2], MOHAMED BAROUDI[1], BOUCHAIB KHAJJI[2], LATIFA FAOUZI[4], MOHAMED ALIA[3], KHALID HERRADI[2], MOHAMED BELAM[1]

[1]Laboratory LMACS, Sultan Moulay Slimane University, MATIC Research Team: Applied Mathematics and Information and Communication Technologie, Department of Mathematics and Computer Science, Khouribga Polydisciplinary Faculty, Morocco

[2]Laboratory of Analysis Modeling and Simulation, Department of Mathematics and Computer Science, Faculty of Sciences Ben M'sik, Hassan II University of Casablanca, Morocco

[3]Laboratory of Mathematics and Population Dynamics (LMPD), Faculty of Sciences Semlalia-Marrakech (FSSM), Cadi Ayyad University, Morocco

[4]Multidisciplinary Laboratory in Educational sciences and Training Engineering, Hight Normal School, Hassan II University, Casablanca, Morocco

Abstract. Diphtheria is a highly infectious and life-threatening disease caused by Corynebacterium diphtheriae, continues to be a significant public health threat, particularly in regions with insufficient vaccination coverage. Despite the progress made in vaccination programs globally, recent outbreaks, such as those in Thailand in 2019 and Guinea in 2023, have highlighted the resurgence of the disease, especially among populations with waning immunity. In this study, we extend the classic Susceptible-Infectious-Recovered (SIR) model to incorporate both deterministic and stochastic time-delayed models, aiming to predict the epidemiological trend of diphtheria and evaluate the impact of multiple control strategies, including vaccination and public awareness campaigns. The

*Corresponding author
E-mail address: sahibissam@email.email
Received October 08, 2024

main contributions of this work include establishing the well-posedness of the proposed models and identifying conditions under which diphtheria may either persist or be eradicated within a population. Parameters for the models were estimated using real-world outbreak data, and numerical simulations were conducted to both forecast the future spread of diphtheria and verify the theoretical findings. Our results emphasize the critical role of maintaining high vaccination coverage and the need for timely public health interventions to effectively control the spread of diphtheria.

Keywords: Diphtheria; mathematical modeling; delayed stochastic differential equations (DSDEs).

2020 AMS Subject Classification: 92D30.

1. INTRODUCTION

Diphtheria is a severe, life-threatening infectious disease caused by the bacterium *Corynebacterium diphtheriae*. Despite significant advances in vaccination programs globally, the disease remains a major public health concern, particularly in countries with lower immunization coverage [1]. Diphtheria is an acute bacterial illness that affects the mucous membranes of the throat and nose, often leading to the production of a thick, gray membrane covering the throat, which can cause difficulty in breathing, heart failure, paralysis, or even death if untreated [2]. Historically, diphtheria outbreaks in the 19th and early 20th centuries had devastating impacts, causing high mortality rates before the development of the diphtheria toxoid vaccine [3, 4]. The disease was largely controlled with widespread vaccination during the mid-20th century, yet in recent years, there has been a resurgence, particularly in developing countries, attributed to decreasing vaccination rates and waning immunity among adults [5, 6].

According to the World Health Organization (WHO), several countries have recently experienced outbreaks of diphtheria, particularly in regions with limited healthcare infrastructure. For instance, a recent outbreak in Thailand in 2019 saw a worrying rise in diphtheria fatalities, with mortality rates increasing from 0.12 to 0.26 per 100,000 individuals [7]. This resurgence has been linked to insufficient vaccination coverage, especially in regions where healthcare resources are scarce, and large portions of the population remain unvaccinated [8]. The situation was further compounded by the rise in infections among otherwise healthy adolescents, whose antibody protection from previous vaccination campaigns had diminished over time [9]. Similar

outbreaks have been observed globally, including the Kankan region of Guinea, where in 2023, the WHO reported 538 infections and 58 fatalities, with a case fatality rate of 11% [10].

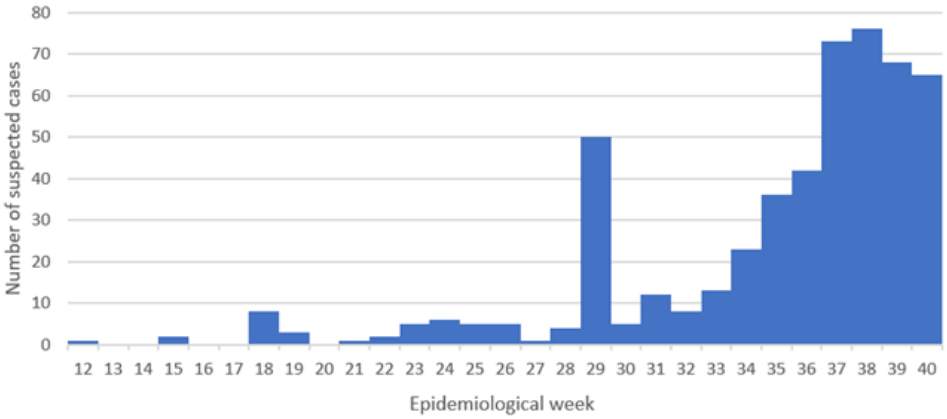

FIGURE 1. Suspected diphtheria cases by epidemiological week in Guinea, as of 13 October 2023 (Source: WHO)

Given the renewed threat posed by diphtheria, understanding its transmission dynamics has become crucial for developing effective control strategies. Diphtheria spreads through respiratory droplets and, in some cases, direct contact with infected individuals or contaminated objects [11]. Asymptomatic carriers, who harbor the bacteria without showing symptoms, also play a significant role in the transmission chain, complicating efforts to curb the disease's spread [12]. The bacterium releases a potent toxin, which leads to cellular damage and can cause severe systemic complications [13]. While vaccination remains the cornerstone of prevention, the growing number of unvaccinated individuals due to vaccine hesitancy, logistical challenges, and gaps in immunization programs threaten to undo decades of progress in disease control [14, 15].

Mathematical modeling has emerged as a vital tool in understanding the dynamics of diphtheria transmission and in forecasting potential outbreaks [16]. These models are instrumental in providing insights into the spread of infectious diseases, allowing researchers and public health officials to simulate various scenarios and evaluate the impact of interventions [17, 18]. For instance, several mathematical models have been developed to assess the effectiveness of different vaccination strategies and the role of asymptomatic carriers in disease transmission [19]. These models, often based on compartmental frameworks such as Susceptible-Infectious-Recovered

(SIR) or Susceptible-Exposed-Infectious-Recovered (SEIR) models, help quantify the basic reproduction number (R_0) of diphtheria in various contexts and predict the trajectory of future outbreaks [20, 21]. For example, one study applied an SEIR model to estimate the impact of waning immunity and incomplete vaccination coverage, highlighting the critical importance of maintaining high vaccination rates to prevent a resurgence of diphtheria [22].

Other studies have integrated stochastic elements into these models to account for environmental fluctuations and the unpredictable nature of human behavior, which can affect vaccination uptake and compliance with public health measures [23]. While deterministic models offer valuable insights into the average behavior of disease outbreaks, stochastic models provide a more realistic representation by incorporating random variables that capture the inherent unpredictability of real-world disease spread [24]. To date, few studies have fully explored the stochastic aspects of diphtheria transmission, underscoring the need for further research in this area [25].

In addition to mathematical modeling, public health strategies have focused on increasing public awareness through education campaigns and improving vaccine coverage in high-risk areas. These strategies are designed to reduce contact between susceptible individuals and those who are asymptomatically infected, thereby decreasing the overall transmission rate [26]. Educational efforts emphasize the importance of vaccination, early detection, and the necessity of seeking medical care promptly when symptoms appear [27, 28]. In several countries, these efforts have led to a resurgence of vaccination campaigns, particularly in regions where healthcare access is limited, such as rural areas in Southeast Asia and sub-Saharan Africa [29].

In this paper, we propose a comprehensive model for diphtheria transmission that incorporates both symptomatic and asymptomatic infections. Unlike previous models, our approach integrates time delays to account for the incubation period and the time required for individuals to become symptomatic, as well as stochastic elements to reflect the environmental uncertainties that affect disease transmission [30]. Our model also distinguishes between different classes of infected individuals, including those who are asymptomatic, symptomatic but untreated, and individuals under quarantine. By including these additional compartments, we aim to provide a more accurate representation of the real-world dynamics of diphtheria spread [31, 32].

Section 2 presents the formulation of the proposed model and its theoretical foundations, followed by a qualitative analysis of its behavior in Section 3. In Sections 4 and 5, we apply the model to data from recent diphtheria outbreaks in Thailand and Guinea, providing parameter estimates and forecasting the potential spread of the disease under various scenarios. Finally, we discuss the implications of our findings for public health policy and offer recommendations for improving vaccination coverage and implementing effective control measures in Section 6.

2. Formulation and Well-Posedness of the Models

Building upon the epidemiological characteristics of diphtheria and the range of strategies implemented by the government to address this pandemic, we adapt the traditional SIR model to describe the spread of diphtheria within Guinea. Specifically, we divide the population into eight categories, represented by $S, I_s, I_a, F_b, F_g, F_c, R, M$ infected individuals showing symptoms; I_a is for those infected without symptoms who have yet to receive treatment; F_b, F_g, F_c denote diagnosed patients who are under the care of the Guinean healthcare system and quarantined, split into three categories: mild, severe, and critical cases. Lastly, R stands for recovered individuals and M represents the fatalities.

The model operates under the following assumptions:

(1) All parameters within the model are constant and positive;
(2) The model disregards natural birth and death rates;
(3) Truly asymptomatic cases will remain asymptomatic until they recover, without contributing to the disease spread;
(4) Patients who are temporarily asymptomatic are classified as symptomatic;
(5) Reinfections are not included in the model;
(6) The Guinea healthcare system is assumed to not be overwhelmed.

The visual representation of the proposed model is shown in Figure (2).

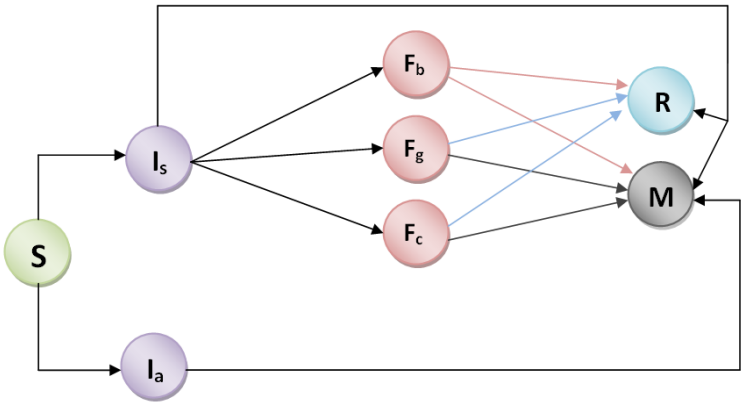

FIGURE 2. Model description.

Following these assumptions and the strategies imposed by Guinean authorities, the spread of diphtheria within the population is governed by the following system of delayed differential equations (DDEs):

$$
(1)\quad \begin{cases}
\dfrac{dS}{dt} = -\alpha(1-v)\dfrac{S(t)I_s(t)}{N}, \\
\dfrac{dI_s}{dt} = \alpha\xi(1-v)\dfrac{S(t-\tau_1)I_s(t-\tau_1)}{N} - \lambda I_s(t) - (1-\lambda)(d_s+\sigma_s)I_s(t), \\
\dfrac{dI_a}{dt} = \alpha(1-\xi)(1-v)\dfrac{S(t-\tau_1)I_s(t-\tau_1)}{N} - \sigma_a I_a(t), \\
\dfrac{dF_b}{dt} = \lambda\pi_b I_s(t-\tau_2) - (d_b+r_b)F_b(t), \\
\dfrac{dF_g}{dt} = \lambda\pi_g I_s(t-\tau_2) - (d_g+r_g)F_g(t), \\
\dfrac{dF_c}{dt} = \lambda\pi_c I_s(t-\tau_2) - (d_c+r_c)F_c(t), \\
\dfrac{dR}{dt} = \sigma_s(1-\lambda)I_s(t-\tau_3) + \sigma_a I_a(t-\tau_3) + r_b F_b(t-\tau_4) + r_g F_g(t-\tau_4) + r_c F_c(t-\tau_4), \\
\dfrac{dM}{dt} = d_s(1-\lambda)I_s(t-\tau_3) + d_b F_b(t-\tau_4) + d_g F_g(t-\tau_4) + d_c F_c(t-\tau_4).
\end{cases}
$$

Let $t \in \mathbb{R}_+$ represent time, and N the total population size, while $v \in [0,1]$ indicates the extent of preventive measures applied to the susceptible population. The parameter λ refers to the disease transmission rate, and $\xi \in [0,1]$ represents the fraction of individuals showing symptoms. The parameter α also defines the portion of symptomatic infected individuals that transitions to the three categories: F_b, F_g, and F_c, with respective rates π_b, π_g, and π_c. The average recovery time for these forms is given by $\frac{1}{r_b}$, $\frac{1}{r_g}$, and $\frac{1}{r_c}$. These forms also exhibit mortality rates of d_b, d_g, and d_c, respectively. For asymptomatic infected individuals who are not diagnosed, they recover at

rate σ_a, while symptomatic infected individuals either recover or die at rates σ_b and d_s. The time delays τ_1, τ_2, τ_3, and τ_4 represent the incubation period, the time before the health system intervenes, and the time elapsed before death for individuals in compartments I_s, F_b, F_g, and F_c. At any given time,

$$D(t) =: d_s(1-\lambda)I_s(t-\tau_3) + d_bF_b(t-\tau_4) + d_gF_g(t-\tau_4) + d_cF_c(t-\tau_4) = \frac{dM(t)}{dt} \tag{2}$$

provides the count of recent deaths caused by the disease

Remark 1.

In the system described by equation (1), the delays occur at the onset, when the infection begins to affect individuals or when healthcare interventions are initiated, rather than at the points where individuals exit the system (recovery or death). For instance, when a susceptible person comes into contact with an infected individual at time t, they become infected at time $t+\tau_1$. At this moment, the compartment representing infected individuals is updated to include this newly infected person. This kind of process is repeated in all other interactions between the compartments in the model, ensuring that all relevant transitions are captured accurately.

Remark 2.

It is assumed that the compartment of symptomatic infected individuals, denoted by I_s, never becomes completely empty at any given time t. In other words, there is always some level of symptomatic infection present in the population. This assumption is reflected in the inequality $d_s + \sigma_s < 1$, which ensures that symptomatic individuals do not fully recover or die within the timeframe. Moreover, the diagnosed symptomatic individuals are categorized into one of three possible stages: F_b, F_g, and F_c, with respective transition rates π_b, π_g, and π_c. These rates reflect the distribution of individuals across the different stages, and they satisfy the condition that their sum is equal to 1, i.e., $\pi_b + \pi_g + \pi_c = 1$, ensuring that the entire population is accounted for.

Remark 3.

From a biological perspective, the delays $\tau_3 = 21$ days and $\tau_4 = 13.5$ days represent the respective time intervals before death for individuals in the I_s compartment and those in the three disease forms F_b, F_g, and F_c. These time delays capture the period it takes for an individual to progress from symptomatic infection to death, and thus are critical for accurately modeling the progression of the disease. These delays are therefore included in the final equation of the

system (1) to ensure that the timing of disease progression is properly accounted for.

Remark 4.

In this study, the time period under consideration is relatively short in comparison to typical demographic timescales. This allows us to make the assumption that there are no new births or immigration (entry into the population), and similarly, no natural deaths or emigration (exit from the population). As such, factors such as recruitment and natural mortality rates can be neglected. Additionally, it is important to note that in this model, individuals who die from the disease remain counted within the population total, meaning that the overall population size, denoted by $N(t)$, is assumed to remain constant over the study period. This assumption is further justified by the fact that Moroccan authorities have closed the country's borders, thereby preventing any significant population movement during the timeframe considered.

The system's initial conditions, denoted as system (1), are given as follows:

$$\begin{aligned} &\psi_1(\varsigma) = S(\varsigma) \geq 0, \quad \psi_2(\varsigma) =) I_s(\varsigma) \geq 0, \quad \psi_3(\varsigma) = I_a(\varsigma) \geq 0, \\ &\psi_4(\varsigma) = F_b(\varsigma) \geq 0, \quad \psi_5(\varsigma) = F_g(\varsigma) \geq 0, \quad \psi_6(\varsigma) = F_c(\varsigma) \geq 0, \\ &\psi_7(\varsigma) = R(\varsigma) \geq 0, \quad \psi_8(\varsigma) = M(\varsigma) \geq 0, \quad \varsigma \in [-\tau, 0], \end{aligned} \tag{3}$$

where $\tau = \max\{\tau_1, \tau_2, \tau_3, \tau_4\}$ represents the longest delay among all the different time delays present in the system. Let $C = C([-\tau, 0], \mathbb{R}^8)$ represent the Banach space of all continuous functions mapping from the interval $[-\tau, 0]$ into $\mathbb{R}^8$, equipped with the uniform topology. According to the fundamental principles of functional differential equations [33], the system (1), initialized with conditions

$$(\varsigma_1, \varsigma_2, \varsigma_3, \varsigma_4, \varsigma_5, \varsigma_6, \varsigma_7, \varsigma_8) \in C,$$

guarantees a unique solution.However, in practical applications, due to ongoing and inevitable fluctuations in the environment, the system's parameters are rarely constant. Instead, they exhibit random variations around some expected average values. Thus, by utilizing delayed stochastic differential equations (DSDEs), we can introduce an enhanced level of realism when compared to purely deterministic models. Parameters such as α and β, which play a critical role in controlling and managing the spread of Diphtheria to various environmental factors. To capture this variability, we incorporate stochastic elements into system (1) by using a technique known as parameter perturbation, which has been employed extensively by numerous

researchers (see, e.g., [34, 35, 36]). In particular, we modify the parameters α and β to introduce random fluctuations as follows: $\alpha \to \alpha + \chi_1 \dot{B}_1(t)$ and $\lambda \to \lambda + \chi_2 \dot{B}_2(t)$, where $B_1(t)$ and $B_2(t)$ are independent standard Brownian motions. These Brownian motions are defined on a complete probability space $(\Omega, \mathscr{F}, \mathbb{P})$, which is equipped with a filtration $\{\mathscr{F}_t\}_{t\geq 0}$ that satisfies the usual assumptions (i.e., it is non-decreasing and $\mathscr{F}_0$ contains all $\mathbb{P}$-null sets). The intensities of the random fluctuations are governed by the constants χ_1 and χ_2, which represent the strength of the noise in the parameters $B_1(t)$ and $B_2(t)$, respectively.

By introducing this stochastic framework, we ensure that the model reflects the inherent uncertainty and randomness in real-world epidemic dynamics. Therefore, the resulting system of delayed stochastic differential equations more accurately represents the unpredictable nature of disease spread in varying environments. Consequently, the modified model can provide more realistic predictions and insights into the behavior of epidemics under fluctuating environmental and social conditions, as compared to deterministic models that assume constant parameters. The new model governed by these delayed stochastic differential equations is as follows:

(4)
$$
\begin{cases}
dS(t) = \left(-\alpha(1-v)\dfrac{S(t)I_s(t)}{N}\right)dt - \chi_1(1-v)\dfrac{S(t)I_s(t)}{N}dB_1(t), \\
dI_s(t) = \left(\alpha\xi(1-v)\dfrac{S(t-\tau_1)I_s(t-\tau_1)}{N} - \lambda I_s(t) - (1-\lambda)(d_s+\sigma_s)I_s(t)\right)dt \\
\quad +\chi_1\left(\xi(1-v)\dfrac{S(t-\tau_1)I_s(t-\tau_1)}{N}\right)dB_1(t) + \chi_2(d_s+\sigma_s-1)I_s(t)dB_2(t), \\
dI_a(t) = \left(\alpha(1-\xi)(1-v)\frac{S(t-\tau_1)I_s(t-\tau_1)}{N} - \sigma_a I_a(t)\right)dt \\
\quad +\chi_1(1-\xi)(1-v)\dfrac{S(t-\tau_1)I_s(t-\tau_1)}{N}dB_1(t), \\
dF_b(t) = (\lambda\pi_b I_s(t-\tau_2) - (d_b+r_b)F_b(t))\,dt + \chi_2\pi_b I_s(t-\tau_2)dB_2(t), \\
dF_g(t) = (\lambda\pi_g I_s(t-\tau_2) - (d_g+r_g)F_g(t))\,dt + \chi_2\pi_g I_s(t-\tau_2)dB_2(t), \\
dF_c(t) = (\lambda\pi_c I_s(t-\tau_2) - (d_c+r_c)F_c(t))\,dt + \chi_2\pi_c I_s(t-\tau_2)dB_2(t), \\
dR(t) = (\sigma_s(1-\lambda)I_s(t-\tau_3) + \sigma_a I_a(t-\tau_3) + r_b F_b(t-\tau_4) + r_g F_g(t-\tau_4) + r_c F_c(t-\tau_4))\,dt \\
\quad -\chi_2\sigma_s I_s(t-\tau_3)dB_2(t), \\
dM(t) = (d_s(1-\lambda)I_s(t-\tau_3) + d_b F_b(t-\tau_4) + d_g F_g(t-\tau_4) + d_c F_c(t-\tau_4))\,dt \\
\quad -\chi_2 d_s I_s(t-\tau_3)dB_2(t).
\end{cases}
$$

The coefficients in the model are assumed to be locally Lipschitz continuous with respect to all variables, for every $t \in \mathbb{R}^+$.

Let us define $\mathbb{R}^8_+$ as:$\mathbb{R}^8_+ = \{(y_1, y_2, y_3, y_4, y_5, y_6, y_7, y_8) \mid y_i > 0,\ i = 1, 2, \ldots, 8\}$. We can now state the following result:

Theorem 1.

For any initial condition that satisfies assumption (3), there exists a unique solution

$$y(t) = (S(t), I_s(t), I_a(t), F_b(t), F_g(t), F_c(t), R(t), M(t))$$

to the stochastic Diphtheria model (4), which remains within $\mathbb{R}^8_+$ with probability one.

Proof.

Since the coefficients in the stochastic differential equations with multiple delays (4) are locally Lipschitz continuous, it follows from [37] that for any square integrable initial condition $y(0) \in \mathbb{R}^8_+$, independent of the given Brownian motion B, there exists a unique local solution $y(t)$ for $t \in [0, \tau_e)$, where τ_e represents the explosion time. To show that this solution is global, it is necessary to demonstrate that $\tau_e = \infty$, meaning the solution remains valid for all time. To prove this, we need to establish that $x(t)$ does not reach infinity within a finite time. Let $k_0 > 0$ be sufficiently large so that $\frac{1}{k_0} < y(0) < k_0$. For each integer $k \geq k_0$, define the stopping time $\tau_k = \inf\left\{t \in [0, \tau_e) : y_i(t) \notin \left(\frac{1}{k}, k\right) \text{ for some } i = 1, 2, 3\right\}$, where the infimum is set to infinity if the condition is never met. It is evident that $\tau_k \leq \tau_e$. Now, let $T > 0$ be arbitrary. We define the following function Z, which is twice differentiable, on $\mathbb{R}^3_+ \to \mathbb{R}^+$:

$$Z(y) = (y_1 + y_2 + y_3)^2 + \frac{1}{y_1} + \frac{1}{y_2} + \frac{1}{y_3}.$$

By applying Itô's lemma, for any $0 \leq t \leq \tau_k \wedge T$ and for all $k \geq 1$, we can write

$$dZ(y(t)) = LZ(y(t))dt + \theta(y(t))dB(t),$$

where θ is a continuous functional, defined on $[0, +\infty) \times C([-\tau, 0], \mathbb{R}^{3\times 2})$, given by

$$\theta(y(t)) = \begin{pmatrix} -\delta_1(1-u)\dfrac{S(t)I_s(t)}{N} & 0 \\ \chi_1\xi(1-v)\dfrac{S(t-\tau_1)I_s(t-\tau_1)}{N} & \chi_2(d_s + \sigma_s - 1)I_s(t) \\ \chi_1(1-\xi)(1-v)\dfrac{S(t-\tau_1)I_s(t-\tau_1)}{N} & 0 \end{pmatrix},$$

and $B(t) = \Big(B_1(t), B_2(t)\Big)^T$, where the superscript "T" denotes the transpose. The operator L represents the differential operator of the function Z, defined by:

$$
\begin{aligned}
LZ(y(t)) &= \left(2(S(t)+I_s(t)+I_a(t)) - \frac{1}{S^2(t)}\right)\left(-\alpha(1-v)\frac{S(t)I_s(t)}{N}\right)\\
&+\left(1+\tfrac{1}{S^3(t)}\right)\left(-\chi_1(1-v)\frac{S(t)I_s(t)}{N}\right)^2\\
&+\left(2(S(t)+I_s(t)+I_a(t)) - \frac{1}{I_s^2(t)}\right)\left(\alpha\xi(1-v)\frac{S(t-\tau_1)I_s(t-\tau_1)}{N} - \lambda I_s(t) - (1-\lambda)(d_s+\sigma_s)I_s(t)\right)\\
&+\left(1+\frac{1}{I_a^3(t)}\right)\left[\left(\chi_1\xi(1-v)\frac{S(t-\tau_1)I_s(t-\tau_1)}{N}\right)^2 + (\chi_2(d_s+\sigma_s-1)I_s(t))^2\right]\\
&+\left(2(S(t)+I_s(t)+I_a(t)) - \frac{1}{I_a^2(t)}\right)\left(\alpha(1-\xi)(1-v)\frac{S(t-\tau_1)I_s(t-\tau_1)}{N} - \sigma_a I_a(t)\right)\\
&+\left(1+\frac{1}{I_a^3(t)}\right)\left(\chi_1(1-\xi)(1-v)\frac{S(t-\tau_1)I_s(t-\tau_1)}{N}\right)^2.
\end{aligned}
$$

Thus, we can conclude:

$$
\begin{aligned}
LZ(y(t)) &\le \frac{\alpha(1-v)S(t)I_s(t)}{NS^2(t)} + \left(1+\frac{1}{S^3(t)}\right)\left(\chi_1(1-v)\frac{S(t)I_s(t)}{N}\right)^2\\
&+2\alpha\xi(1-v)\left(S(t)+I_s(t)+I_a(t)\right)\frac{S(t-\tau_1)I_s(t-\tau_1)}{N} + \frac{\lambda+(1-\lambda)(d_S+\sigma_S)}{I_s(t)}\\
&+\left(1+\frac{1}{I_s^3(t)}\right)\left[\left(\chi_1\xi(1-v)\frac{S(t-\tau_1)I_s(t-\tau_1)}{N}\right)^2 + (\chi_2(d_s+\sigma_s-1)I_s(t))^2\right]\\
&+2\alpha(1-\xi)(1-v)\left(S(t)+I_s(t)+I_a(t)\right)\frac{S(t-\tau_1)I_s(t-\tau_1)}{N}\\
&+\frac{\sigma_a}{I_a(t)} + \left(1+\frac{1}{I_a^3(t)}\right)\left(\chi_1(1-\xi)(1-v)\frac{S(t-\tau_1)I_s(t-\tau_1)}{N}\right)^2.
\end{aligned}
\tag{5}
$$

We now apply the basic inequality $2xz \le x^2+z^2$, which is valid for any $x,z\in\mathbb{R}$. First, we take $x=\alpha\xi(1-v)$ and $z=S(t)+I_s(t)+I_a(t)$, and then we take $x=\alpha(1-\xi)(1-v)$ and $z=S(t)+I_s(t)+I_a(t)$. By doing so, we can simplify the right-hand side of inequality (5) to obtain:

$$
\begin{aligned}
LZ(y(t)) &\le a_1 + \psi(S(t)+I_s(t)+I_a(t))^2 + \frac{a_2}{S(t)} + \frac{a_3}{I_s(t)} + \frac{a_4}{I_a(t)},\\
&\le M(1+Z(y(t))),
\end{aligned}
$$

where ψ, a_1, a_2, a_3, a_4 are positive constants, and $M=\max(\psi,a_1,a_2,a_3,a_4)$. By integrating both sides of the inequality, we get the desired result.

$$dZ(y(t)) = LW(y(t))dt + \theta(y(t))dB(t)$$

over the interval from t_0 to $t \wedge \tau_k$. Since the expectation removes the martingale component, we have:

$$E(Z(y(t \wedge \tau_k))) = E(W(y_0)) + E\int_{t_0}^{t\wedge\tau_k} LZ(y(s))ds$$

$$\leq E(Z(y_0)) + E\int_{t_0}^{t\wedge\tau_k} M(1+Z(y(s)))ds$$

$$\leq E(Z(y_0)) + MT + \int_{t_0}^{t\wedge\tau_k} E(Z(y(s)))ds.$$

By Gronwall's inequality, it follows that:

$$E(Z(y(t \wedge \tau_k))) \leq (E(Z(y_0)) + MT)\exp(CT).$$

Now, for $\omega \in \{\tau_k \leq T\}$, the value of $y_i(\tau_k)$ is either k or $\frac{1}{k}$ for some $i = 1,2,3$. Hence,

$$Z(y_i(\tau_k)) \geq \left(k^2 + \frac{1}{k}\right) \wedge \left(\frac{1}{k^2} + k\right).$$

Therefore, we have:

$$(EZ(y_0) + MT)\exp(CT) \geq E\left(\mathbb{X}_{\{\tau_k \leq T\}}(\omega) Z(x_{\tau_k})\right)$$

$$\geq \left(k^2 + \frac{1}{k}\right) \wedge \left(\frac{1}{k^2} + k\right) P(\tau_k \leq T).$$

By letting $k \to \infty$, it follows that $P(\tau_e \leq T) = 0$. Since T is arbitrary, we conclude that $P(\tau_e = \infty) = 1$.

Next, we define the stopping time $\tilde{\tau}_k$ as

$$\tilde{\tau}_k = \inf\left\{t \in [0, \tau_e) : x_i(t) \notin \left(\frac{1}{k}, k\right) \text{ for some } i = 4, \ldots, 8\right\},$$

and consider the twice-differentiable function $\tilde{Z}$ on $\mathbb{R}^5_+ \to \mathbb{R}^+$, defined as:

$$\tilde{Z}(y) = \left(\sum_{i=4}^{8} y_i\right)^2 + \sum_{i=4}^{8} \frac{1}{y_i'},$$

and, following the same procedure, we conclude that all variables of the system are positive over the interval $[0, \infty)$. □

3. Qualitative Analysis of the Models

The basic reproduction number, often used to quantify the transmission potential of a disease within a population, is a critical measure in determining the trajectory of an outbreak [38]. It represents the average number of secondary infections generated by a single infectious individual in a completely susceptible population. It's important to note that the basic reproduction number, denoted as R_0, is determined by the parameters of the model and is independent of the state variables of the system. Additionally, the calculation of R_0 in this model does not depend on the time delays. To calculate R_0, we employ the next-generation matrix approach described in [39]. Specifically, for the system in equation (1), the basic reproduction number is given by:

$$R_0 = \rho(FV^{-1}) = \frac{\alpha\xi(1-v)}{(1-\lambda)(\sigma_s+d_s)+\lambda'}. \tag{6}$$

Here, ρ represents the spectral radius of the next-generation matrix FV^{-1}, where the matrices F and V are defined as follows:

$$F = \begin{pmatrix} \alpha\xi(1-v) & 0 \\ 0 & 0 \end{pmatrix}, \quad V = \begin{pmatrix} (1-\lambda)(\sigma_s+d_s)+\lambda & 0 \\ 0 & \sigma_a \end{pmatrix}.$$

Observing that the compartments which directly contribute to the disease transmission are I_s, I_a, F_b, F_g, and F_c, we can reduce the analysis of the local stability of system (1) to the local stability of the following system:

$$\begin{cases} \dfrac{dI_s(t)}{dt} = \alpha\xi(1-v)\dfrac{S(t-\tau_1)I_s(t-\tau_1)}{N} - \lambda I_s(t) - (1-\lambda)(d_s+\sigma_s)I_s(t), \\ \dfrac{dI_a(t)}{dt} = \alpha(1-\xi)(1-v)\dfrac{S(t-\tau_1)I_s(t-\tau_1)}{N} - \sigma_a I_a(t), \\ \dfrac{dF_b(t)}{dt} = \lambda\pi_b I_s(t-\tau_2) - (d_b+r_b)F_b(t), \\ \dfrac{dF_g(t)}{dt} = \lambda\pi_g I_s(t-\tau_2) - (d_g+r_g)F_g(t), \\ \dfrac{dF_c(t)}{dt} = \lambda\pi_c I_s(t-\tau_2) - (d_c+r_c)F_c(t). \end{cases} \tag{7}$$

The remaining compartments are decoupled from the system, and since the total population size N is constant, we can derive the following analytical expressions:

(8)
$$\begin{cases} dS(t) = N - (I_s(t) + I_a(t) + F_b(t) + F_g(t) + F_c(t) + R(t) + M(t)), \\ R(t) = \int_0^t [\sigma_s(1-\lambda)I_s(\upsilon-\tau_3) + \sigma_a I_a(\upsilon-\tau_3) + r_b F_b(\upsilon-\tau_4) + r_g F_g(\upsilon-\tau_4) + r_c F_c(\upsilon-\tau_4)]d\upsilon, \\ M(t) = \int_0^t [d_s(1-\lambda)I_s(\upsilon-\tau_3) + d_a I_a(\upsilon-\tau_3) + d_b F_b(\upsilon-\tau_4) + d_g F_g(\upsilon-\tau_4) + d_c F_c(\upsilon-\tau_4)]d\upsilon. \end{cases}$$

Let $\bar{E} = (\bar{I}_S, \bar{I}_a, \bar{F}_b, \bar{F}_g, \bar{F}_c)$ represent an arbitrary equilibrium, and consider the system (7). Introducing the following change of variables:

$$N_1(t) = I_s(t) - I_s^r, \quad N_2(t) = I_a(t) - I_a^r, \quad N_3(t) = F_b(t) - F_b^r, \quad N_4(t) = F_g(t) - F_g^r, \quad N_5(t) = F_c(t) - F_c^r.$$

By substituting $N_i(t), i = 1,2,\ldots,5$ into system (7) and linearizing around the equilibrium, we obtain a new system equivalent to:

$$\frac{dH(t)}{dt} = AH(t) + BH(t-\tau_1) + CH(t-\tau_2), \tag{9}$$

where $H(t) = (N_1(t), N_2(t), N_3(t), N_4(t), N_5(t))^T$ and A, B, C are the Jacobian matrices of system (7). The Jacobian matrix A for system (7) is given as:

$$A = \begin{pmatrix} -\lambda - (1-\lambda)(d_S + \sigma_S) & 0 & 0 & 0 & 0 \\ 0 & -\sigma_a & 0 & 0 & 0 \\ 0 & 0 & -(d_b + r_b) & 0 & 0 \\ 0 & 0 & 0 & -(d_g + r_g) & 0 \\ 0 & 0 & 0 & 0 & -(d_c + r_c) \end{pmatrix},$$

The matrix B corresponding to the delayed terms in system (9) is represented as:

$$B = \begin{pmatrix} \alpha\xi(1-v) & 0 & 0 & 0 & 0 & 0 \\ \alpha(1-\xi)(1-v) & 0 & 0 & 0 & 0 & 0 \\ 0 & 0 & 0 & 0 & 0 & 0 \\ 0 & 0 & 0 & 0 & 0 & 0 \\ 0 & 0 & 0 & 0 & 0 & 0 \end{pmatrix},$$

And the matrix C, which corresponds to the second delay τ_2, is expressed as:

$$C = \begin{pmatrix} 0 & 0 & 0 & 0 & 0 \\ 0 & 0 & 0 & 0 & 0 \\ \lambda r_b & 0 & 0 & 0 & 0 \\ \lambda r_g & 0 & 0 & 0 & 0 \\ \lambda r_c & 0 & 0 & 0 & 0 \end{pmatrix}.$$

The characteristic equation for system (7) can be expressed as:

$$P(\varepsilon) = (\varepsilon - b_1(R_0 e^{-\varepsilon\tau_1} - 1))(\varepsilon + \sigma_a)(\varepsilon + (d_b + r_b))(\varepsilon + (d_g + r_g))(\varepsilon + (d_c + r_c)), \tag{10}$$

where

$$b_1 = \lambda + (1-\lambda)(d_S + \sigma_S).$$

The characteristic equation (10) clearly has the following roots: $\varepsilon_1 = -\sigma_a$, $\varepsilon_2 = -(d_b + r_b)$, $\varepsilon_3 = -(d_g + r_g)$, $\varepsilon_4 = -(d_c + r_c)$ and the root of the equation:

$$\varepsilon - b_1(R_0 e^{-\varepsilon\tau_1} - 1) = 0. \tag{11}$$

Now, suppose $\mathrm{Re}(\varepsilon) \geq 0$. From (11), we obtain:

$$\mathrm{Re}(\varepsilon) = b_1(R_0 e^{-\varepsilon\tau_1}\cos(\mathrm{Im}\varepsilon\tau_1) - 1) < 0,$$

if $R_0 < 1$, which contradicts $\mathrm{Re}(\varepsilon) \geq 0$. On the other hand, we show that equation (11) has a positive real root when $R_0 > 1$. Indeed, let us define:

$$\Phi(\varepsilon) = \varepsilon - b_1(R_0 e^{-\varepsilon\tau_1} - 1).$$

We know that $\Phi(0) = -b_1(R_0 - 1) < 0$, and as $\varepsilon \to +\infty$, $\Phi(\lambda) \to +\infty$. Furthermore, Φ is continuous on the interval $(0, +\infty)$. Therefore, Φ has a positive root, and the following result holds.

Theorem 2.

The disease-free equilibrium of system (1), i.e., $(N,0,0,0,0,0,0)$*, is locally asymptotically stable if* $R_0 < 1$ *and unstable if* $R_0 > 1$.

Knowing the deterministic threshold R_0 *is crucial in determining the dynamic behavior of system (1), as it predicts whether the disease will persist or eventually die out. Similarly, we can*

characterize the behavior of system (4) by imposing a sufficient condition for the eradication of the disease.

Theorem 3.

Let $y(t) = (S(t), I_s(t), I_a(t), F_b(t), F_g(t), F_c(t), R(t), M(t))$ represent the solution to the Diphteria stochastic model (4), starting from initial condition $y(0)$. Assume that:

$$\chi_1^2 > \frac{\alpha^2}{2(\lambda + (1-\lambda)(d_S + \sigma_S))}.$$

Then,

$$\limsup_{t \to +\infty} \frac{\ln I_s(t)}{t} < 0. \tag{12}$$

Thus, $I_s(t)$ tends to zero exponentially almost surely, which means the disease dies out with probability one.

Proof.

Let us define:

$$\begin{aligned}
\frac{d \ln I_s(t)}{dt} &= \frac{1}{I_s(t)} \left[\alpha \xi (1-v) \frac{S(t-\tau_1) I_s(t-\tau_1)}{N} - \lambda I_s(t) - (1-\lambda)(d_s + \sigma_s) I_s(t) \right] \\
&+ \frac{1}{2 I_s^2(t)} \left((\chi_1 \xi (1-v) \frac{S(t-\tau_1) I_s(t-\tau_1)}{N})^2 + (\chi_2 (d_s + \sigma_s - 1) I_s(t))^2 \right) \\
&+ \chi_1 \alpha \xi (1-v) \frac{S(t-\tau_1) I_s(t-\tau_1)}{N I_s(t)} dB_1(t) + \chi_2 (d_s + \sigma_s - 1) I_s(t) dB_2(t).
\end{aligned}$$

To simplify the expression, let us define:

$$\begin{aligned}
K(t) &= \xi (1-v) \frac{S(t-\tau_1) I_s(t-\tau_1)}{N}, \quad K_1(t) = \chi_1 \frac{G(t)}{I_s(t)}, \\
K_3 &= \chi_2 (d_s + \sigma_s - 1), \quad K_2 = -\lambda - (1-\lambda)(d_s + \sigma_s).
\end{aligned}$$

With these definitions, we obtain:

$$\begin{aligned}
d \ln I_s(t) &= \left[\frac{\alpha K(t)}{I_s(t)} + K_2 + \frac{1}{2} \left(\left(\frac{\chi_1 K(t)}{I_s(t)} \right)^2 + K_3^2 \right) \right] dt + K_1(t) dB_1(t) + K_3 dB_2(t), \\
&= \left[-\frac{\chi_2^2}{2} \left[\frac{K^2(t)}{I_s^2(t)} - \frac{2\alpha^2}{\chi_1^2} \frac{K(t)}{I_s(t)} \right] + K_2 - \tfrac{K_3^2}{2} \right] dt + K_1(t) dB_1(t) + K_3 dB_2(t), \\
&= \left[-\frac{\chi_2^2}{2} \left[\left(\frac{K(t)}{I_s(t)} - \frac{\alpha}{\chi_1^2} \right)^2 - \frac{\alpha^2}{\chi_1^4} \right] + K_2 - \frac{K_3^2}{2} \right] dt + K_1(t) dB_1(t) + K_3 dB_2(t), \\
&\leq \left[\frac{\alpha^2}{2\chi_1^2} + K_2 \right] dt + K_1(t) dB_1(t) + K_3 dB_2(t).
\end{aligned}$$

By integrating both sides of the above inequality over the interval $[0,t]$, we get:

$$\frac{\ln I_s(t)}{t} \leq \frac{\ln I_s(0)}{t} + \frac{\alpha^2}{2\chi_1^2 t} + K_2 + \frac{T_1(t)}{t} + \frac{T_3(t)}{t},$$

where

$$T_1(t) = \int_0^t RK1(s)dB_1(s), \quad T_3(t) = \int_0^t K_3 dB_2(s).$$

We now compute the upper bounds for $T_1(t)$ and $T_3(t)$. First, consider:

$$\begin{aligned}\langle T_1, T_1\rangle_t &= \int_0^t \chi_1^2 \xi^2 (1-v)^2 \frac{S(t-\tau_1)^2 I_s(t-\tau_1)^2}{N^4 I_s^2(t)} ds \\ &\leq \int_0^t \chi_1^2 \xi^2 (1-v)^2 \frac{N^4}{I_s^2(t)} ds \\ &\leq \int_0^t \chi_1^2 \xi^2 (1-v)^2 ds.\end{aligned}$$

Thus,

$$\lim\sup_{t\to+\infty} \frac{\langle T_1, T_1\rangle_t}{t} \leq \chi_1^2 \xi^2 (1-v)^2 < +\infty.$$

From the martingale convergence theorem [40], we conclude that:

$$\lim_{t\to+\infty} \frac{T_1(t)}{t} = 0.$$

Similarly, for $T_3(t)$, we have:

$$\langle T_3, T_3\rangle_t = \int_0^t \chi_3^2 (d_S + \sigma_S)^2 ds = \chi_3^2 (d_S + \sigma_S)^2 t.$$

Thus,

$$\lim\sup_{t\to+\infty} \frac{\langle T_3, T_3\rangle_t}{t} \leq \chi_3^2 (d_S + \sigma_S) < +\infty,$$

and we conclude that:

$$\lim_{t\to+\infty} \frac{T_3(t)}{t} = 0.$$

Subsequently,

$$\lim\sup_{t\to+\infty} \frac{\ln I_s(t)}{t} \leq \frac{\alpha^2}{2\chi_1^2} - \lambda - (1-\lambda)(d_S + \sigma_S).$$

Thus, if

$$\frac{\alpha^2}{2\chi_1^2} - \lambda - (1-\lambda)(d_S + \sigma_S) < 0,$$

then

$$\lim_{t\to+\infty} I_s(t) = 0.$$

This concludes the proof. □ □

4. PARAMETER ESTIMATION

Determining the parameters for the model presents a significant challenge due to the rapidly changing nature of the Diphteria pandemic and the variation in government policies across different regions. Parameters evolve over time as new policies are implemented on a daily basis. To account for this variability and simulate the Diphteria models (1) and (4), we select some parameters from the literature while others are estimated or fitted.

Since the transmission rate α is unknown, we apply the least-squares method to estimate it based on real-time confirmed cases reported in Morocco from 2 March to 13 October 2023 [41]. Using this approach, we estimate α to be 0.4258 (85% CI, 0.3373–0.546). The average infectious period for symptomatic individuals is approximately 21 days, with a crude mortality rate of 3% to 4% [42]. Accordingly, we set $d_S = 0.01/21$ per day, and $\sigma_S = 0.8/21$ per day. Additionally, given that hospitals are not yet overwhelmed, we assume a mortality rate of 43% for critically ill patients, with an average stay of 12.5 days [42]. Therefore, we choose $d_c = 0.4/13.5$ per day and $r_c = 0.6/13.5$ per day. According to the study in [42], the proportion of asymptomatic individuals ranges from 20.6% to 39.9%, while symptomatic cases account for 60.1% to 79.4% of the infected population. The progression rates r_b, r_g, and r_c, from mild to more severe forms of the disease, are assumed to be 70% for mild cases, 20% for severe cases, and 10% for critical cases [42]. The incubation period is assumed to be 5.5 days [43], while the average time before hospitalization is estimated to be 7.5 days [44]. Based on clinical observations in Guinea, we estimate that the evolution of asymptomatic individuals leads to recovery or death after 21 days if there are no other underlying clinical issues. When clinical intervention is applied, the critical cases either recover or result in death after 13.3 days. The remaining parameter values are provided in Table (1).

Parameter	**Value**	**Source**	**Parameter**	**Value**	**Source**
α	0.4517	Estimated	v	[0–1]	Varied
ξ	0.794	[42]	π_b	0.8	[42]
π_g	0.15	[42]	π_c	0.05	[42]
λ	0.06	Assumed	σ_a	1/21	Calculated
σ_s	0.8/21	Calculated	d_s	0.01/21	Calculated
d_b	0	Assumed	d_g	0	Assumed
d_c	0.4/13.5	Calculated	r_b	1/13.5	Calculated
r_g	1/13.5	Calculated	r_c	0.6/13.5	Calculated
τ_1	5.5	[43]	τ_2	7.5	[44]
τ_3	21	Assumed	τ_4	13.5	Assumed
χ_1	1.03	Calculated	χ_2	0.1	Assumed

TABLE 1. Parameter values of models (1) and (4).

5. NUMERICAL SIMULATION OF GUINEAN DIPHTERIA EVOLUTION

In this section, we present the simulations of Diphteria spread in Guinea under different strategies implemented by the Guinean authorities. Considering the four stages of preventive measures implemented to limit the spread of the virus, we estimate the effectiveness of these Guinean interventions as follows:

$$v = \begin{cases} 0.2, & \text{on (2 March, 10 March);} \\ 0.3, & \text{on (10 March, 20 March);} \\ 0.4, & \text{on (20 March, 6 April);} \\ 0.8, & \text{after 6 April.} \end{cases}$$

In Figure (3), it is clear that the graphical representations and clinical data demonstrate a global consistency.

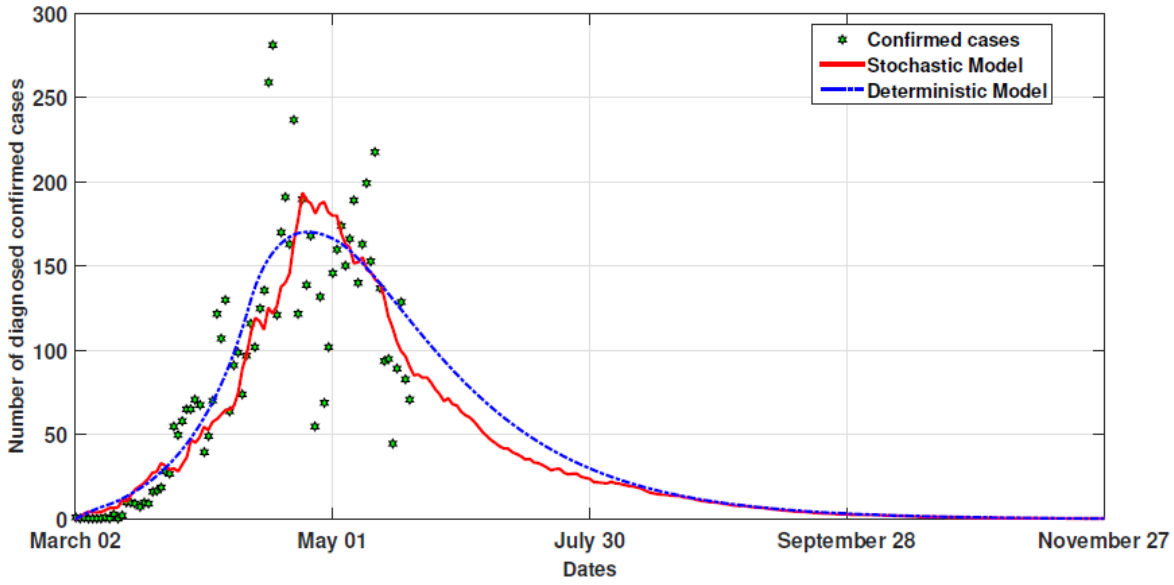

FIGURE 3. Comparison of the deterministic and the stochastic dynamical behavior with the daily reported cases of Diphteria in Guinea.

Additionally, the most recent daily case reports in Guinea [41] align with the biological trend predicted by our model. Therefore, our models are effective in capturing the spread of Diphteria in Guinea. However, it is important to note that some clinical data deviate from the model's predictions, likely due to specific outbreaks occurring in larger regions or in certain industrial zones.

Furthermore, we observe that the stochastic dynamics of Diphteria display particular characteristics when compared to the deterministic model. Specifically, the peak of the stochastic model is more pronounced, and the time to eradication is shorter. At the same time, the conditions outlined in Theorems (2) and (3) are met. To be more precise, the basic reproduction number $R_0 = 0.5230$ is less than one as of 12 October 2023, and $\chi_1^2 = 1.0583 > 1.0497 = \dfrac{\alpha^2}{2\lambda(1-\lambda)(d_S+\sigma_S)}$, ensuring that the disease will eventually be eradicated.

To illustrate the biological relevance of the delay parameters, we present Figure (4), which displays the evolution of diagnosed positive cases, comparing the scenarios with and without delay effects.

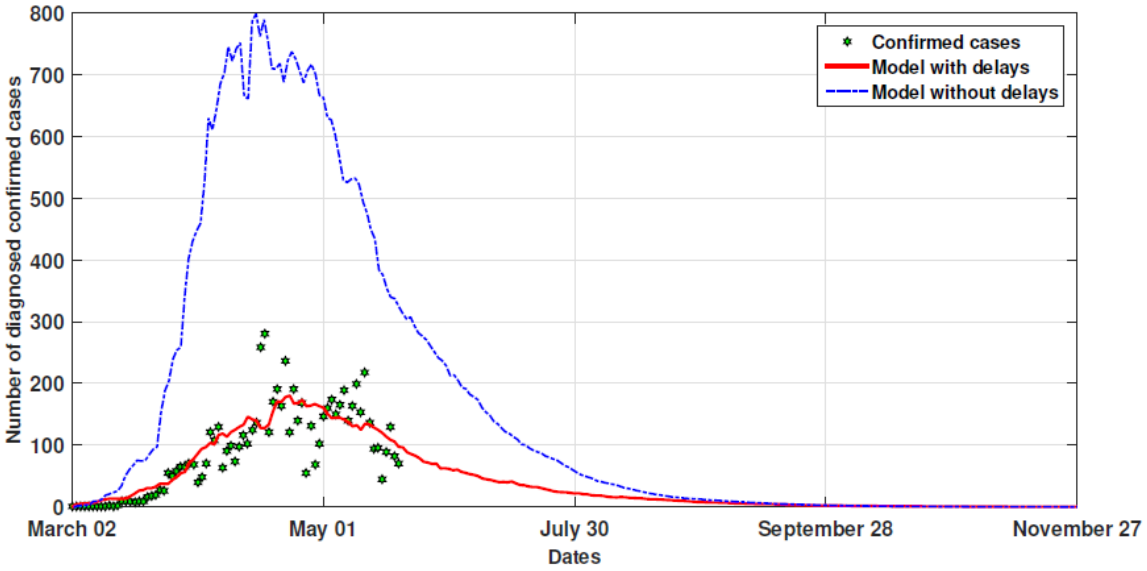

FIGURE 4. Effect of delays on the diagnosed confirmed cases.

In Figure (4), we observe that delays significantly affect the number of diagnosed positive cases. When we compare the plot of model (4) without delays ($\tau = 0, i = 1,2,3,4$) to the clinical data, we notice that the two differ substantially. This suggests that delays play a critical role in understanding the dynamics of Diphteria, particularly in Guinea. By considering these delays, we gain a clearer picture of the disease's behavior and can better comprehend its global impact.

In Figure (5), we provide predictions for the number of susceptible individuals, as well as the forecast for deaths, severe cases, and critical forms. From these figures, it can be deduced that Diphteria will not infect the entire population.

Furthermore, the number of required hospital beds or ventilators can be estimated based on the predicted numbers for each clinical form. It is also noteworthy that the number of deaths predicted by our model is lower than that reported in other countries [45], which indicates that Guinea has successfully avoided a severe epidemic by enforcing the recommended strategies.

Lastly, in Figure (6), we present the cumulative diagnosed cases, severe cases, critical cases, and deaths over 240 days from the start of the Diphteria pandemic in Guinea. Table (2) summarizes key numbers, providing insights into the future trajectory of the epidemic in Guinea.

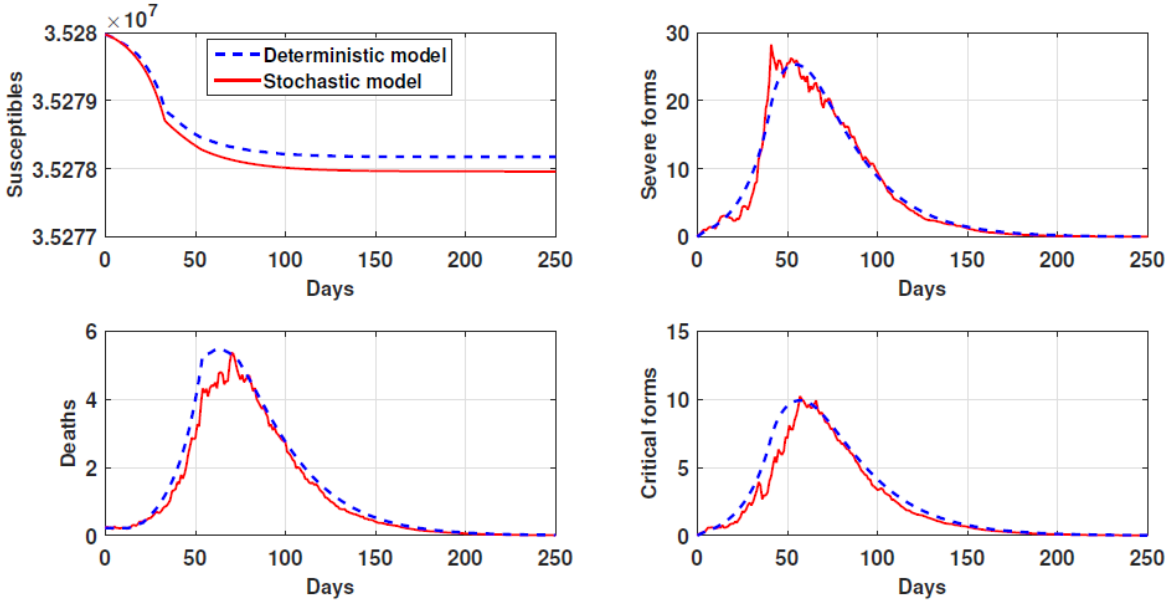

FIGURE 5. The evolution of susceptible individuals, deaths, severe cases, and critical cases from 13 October 2023.

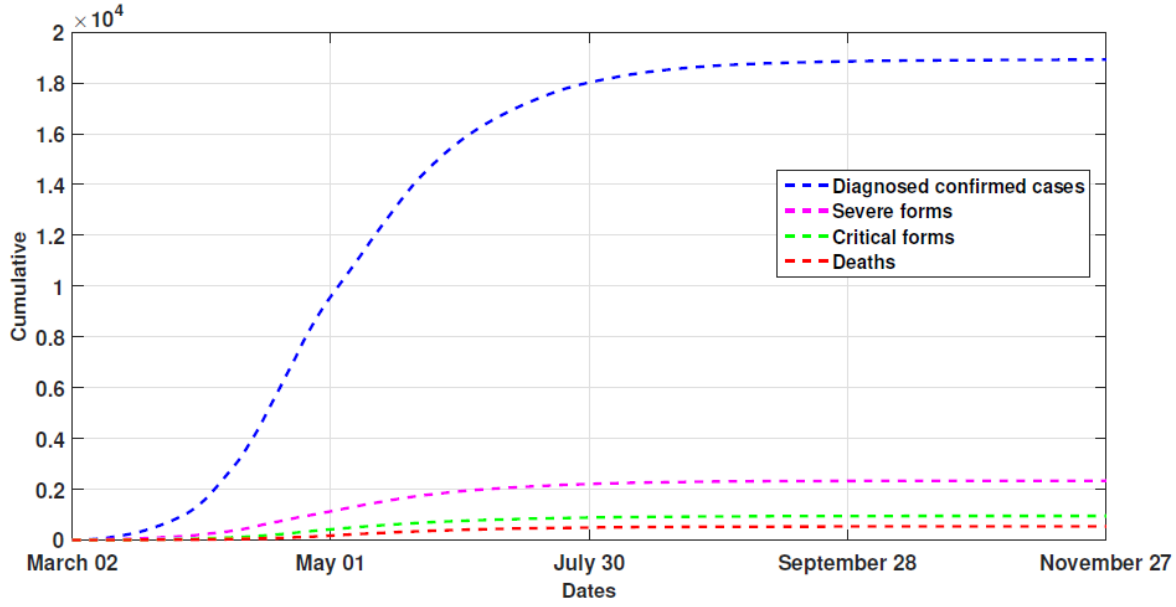

FIGURE 6. Cumulative diagnosed cases, severe forms, critical forms, and deaths over a 240-day period starting from the beginning of the pandemic in Guinea.

TABLE 2. Estimated peaks and cumulative of diagnosed cases, severe forms, critical forms and deaths.

Compartments	Peak	Cumulative
Diagnosed	Around 190	18,890
Severe forms	Around 28	2233
Critical forms	Around 10	997
Deaths	Around 5	468

6. CONCLUSION

In this paper, we developed a comprehensive model to describe the transmission dynamics of diphtheria, incorporating both symptomatic and asymptomatic infections, as well as stochastic elements to account for environmental uncertainties. We proved that our model is both mathematically and biologically well-posed by demonstrating the existence and uniqueness of positive solutions. Additionally, we analyzed the stability of the disease-free equilibrium and established conditions under which the disease would become extinct when the basic reproduction number R_0 is less than one.

By utilizing parameter values obtained from literature and recent outbreak data from Thailand and Guinea, we provided numerical simulations that allowed us to predict the trajectory of diphtheria outbreaks under various scenarios. These simulations highlighted the critical role of maintaining high vaccination rates and addressing gaps in immunization programs to prevent future resurgences of the disease.

Our findings emphasize the importance of integrating both deterministic and stochastic approaches in disease modeling to provide a more accurate depiction of real-world dynamics. Furthermore, the results underline the necessity of proactive public health interventions, including vaccination campaigns and public awareness programs, to mitigate the spread of diphtheria, particularly in regions with limited healthcare infrastructure.

As future work, we intend to explore the spatial spread of diphtheria in affected regions and assess the effectiveness of regional control strategies. This extension will provide additional insights into the impact of geographical factors on disease transmission and help optimize public health responses.

CONFLICT OF INTERESTS

The authors declare that there is no conflict of interests.

REFERENCES

[1] M.V. Murhekar, Resurgence of diphtheria in India, J. Infect. 80 (2020), 232–254. https://doi.org/10.1016/j.jinf.2019.10.010.

[2] L. Brenzel, L.J. Wolfson, J. Fox-rushby, et al. Vaccine-preventable diseases, in: Disease Control Priorities in Developing Countries. 2nd Edn. Washington, D.C.: World Bank, pp. 389–412, 2006.

[3] D.M. Anderson, K.K. Charles, M. McKelligott, et al. Safeguarding consumers through minimum quality standards: milk inspections and urban mortality, 1880-1910, IZA Discussion Paper No. 15295, (2022). https://doi.org/10.2139/ssrn.4114880.

[4] B. Greenwood, The contribution of vaccination to global health: past, present and future, Phil. Trans. R. Soc. B: Biol. Sci. 369 (2014), 20130433. https://doi.org/10.1098/rstb.2013.0433.

[5] K.E.N. Clarke, Review of the epidemiology of diphtheria 2000-2016, World Health Organization, (2017).

[6] B.A. Lopman, V.E. Pitzer, Waxing understanding of waning immunity, J. Infect. Dis. 217 (2018), 851–853. https://doi.org/10.1093/infdis/jix670.

[7] World Health Organization, Diphtheria situation reports, WHO Press, 2020.

[8] H. Martini, O. Soetens, D. Litt, et al. Diphtheria in Belgium: 2010–2017, J. Med. Microbiol. 68 (2019), 1517–1525. https://doi.org/10.1099/jmm.0.001039.

[9] J.G. Wood, N. Goeyvaerts, C.R. MacIntyre, R.I. Menzies, P.B. McIntyre, N. Hens, Estimating vaccine coverage from serial trivariate serologic data in the presence of waning immunity, Epidemiology 26 (2015), 381–389. https://doi.org/10.1097/EDE.0000000000000278.

[10] U. Samarasekera, Diphtheria outbreak in West Africa, Lancet Infect. Dis. 24 (2024), e87. https://doi.org/10.1016/S1473-3099(24)00026-4.

[11] Z. Islam, S. Ahmed, M.M. Rahman, et al. Global stability analysis and parameter estimation for a diphtheria model: a case study of an epidemic in rohingya refugee camp in Bangladesh, Comput. Math. Methods Med. 2022 (2022), 6545179. https://doi.org/10.1155/2022/6545179.

[12] O.S. Johnson, H.O. Edogbanya, A. Wakili, et al. Diphtheria disease transmission dynamics in low vaccine coverage setting, Int. J. Math. Sci. Optim.: Theory Appl. 10 (2024), 79–106.

[13] R.J. Collier, Diphtheria toxin: mode of action and structure, Bacteriol. Rev. 39 (1975), 54–85. https://doi.org/10.1128/br.39.1.54-85.1975.

[14] G.E. Reynolds, H. Saunders, A. Matson, et al. Public health action following an outbreak of toxigenic cutaneous diphtheria in an Auckland refugee resettlement centre, Commun. Dis. Intell. Q. Rep. 40 (2016), E475–E481.

[15] A.B. Wiyeh, S. Cooper, C.A. Nnaji, et al. Vaccine hesitancy 'outbreaks': using epidemiological modeling of the spread of ideas to understand the effects of vaccine related events on vaccine hesitancy, Expert Rev. Vaccines 17 (2018), 1063–1070. https://doi.org/10.1080/14760584.2018.1549994.

[16] W.M. Sweileh, Global research activity on mathematical modeling of transmission and control of 23 selected infectious disease outbreak, Glob. Health 18 (2022), 4. https://doi.org/10.1186/s12992-022-00803-x.

[17] J. Tolles, T. Luong, Modeling epidemics with compartmental models, JAMA 323 (2020), 2515–2516. https://doi.org/10.1001/jama.2020.8420.

[18] A. Smirnova, L. deCamp, G. Chowell, Forecasting epidemics through nonparametric estimation of time-dependent transmission rates using the SEIR model, Bull. Math. Biol. 81 (2019), 4343–4365. https://doi.org/10.1007/s11538-017-0284-3.

[19] S. Bolotin, E.T. Harvill, N.S. Crowcroft, What to do about pertussis vaccines? linking what we know about pertussis vaccine effectiveness, immunology and disease transmission to create a better vaccine, Pathog. Dis. 73 (2015), ftv057. https://doi.org/10.1093/femspd/ftv057.

[20] C.E. Madubueze, K.A. Tijani, Fatmawati, A deterministic mathematical model for optimal control of diphtheria disease with booster vaccination, Healthc. Anal. 4 (2023), 100281. https://doi.org/10.1016/j.health.2023.100281.

[21] R. Matsuyama, A.R. Akhmetzhanov, A. Endo, et al. Uncertainty and sensitivity analysis of the basic reproduction number of diphtheria: a case study of a rohingya refugee camp in Bangladesh, November–december 2017, PeerJ 6 (2018), e4583. https://doi.org/10.7717/peerj.4583.

[22] S.E. Talbird, E.M. La, J. Carrico, et al. Impact of population aging on the burden of vaccine-preventable diseases among older adults in the united states, Hum. Vaccin. Immunother. 17 (2021), 332–343. https://doi.org/10.1080/21645515.2020.1780847.

[23] R.F. Engle, A.D. Smith, Stochastic permanent breaks, Rev. Econ. Stat. 81 (1999), 553–574. https://doi.org/10.1162/003465399558382.

[24] R. Manjoo-Docrat, A spatio-stochastic model for the spread of infectious diseases, J. Theor. Biol. 533 (2022), 110943. https://doi.org/10.1016/j.jtbi.2021.110943.

[25] S. Funk, A. Camacho, A.J. Kucharski, et al. Real-time forecasting of infectious disease dynamics with a stochastic semi-mechanistic model, Epidemics 22 (2018), 56–61. https://doi.org/10.1016/j.epidem.2016.11.003.

[26] World Health Organization, Diphtheria vaccine: who position paper, august 2017 – recommendations, Vaccine 36 (2018), 199–201. https://doi.org/10.1016/j.vaccine.2017.08.024.

[27] M.O. Oduoye, Z.M. Musa, A.M. Tunde, et al. The recent outbreak of diphtheria in nigeria is a public health concern for all, Int. J. Surgery: Glob. Health 6 (2023), e0274. https://doi.org/10.1097/GH9.0000000000000274.

[28] J.P. Uwizihiwe, 40th anniversary of introduction of expanded immunization program (epi): a literature review of introduction of new vaccines for routine childhood immunization in sub-saharan Africa, Int. J. Vaccines Vaccin. 1 (2015), 14–30. https://doi.org/10.15406/ijvv.2015.01.00004.

[29] World Health Organization, Global vaccine coverage reports, WHO Press, 2019.

[30] C.J. Dibble, E.B. O'Dea, A.W. Park, J.M. Drake, Waiting time to infectious disease emergence, J. R. Soc. Interface 13 (2016), 20160540. https://doi.org/10.1098/rsif.2016.0540.

[31] E.B. Akponana, E.O. Arierhie, N.J. Egbune, et al. Mathematical modelling of diphtheria transmission dynamics for effective strategies of prevention and control with emphasis on vaccination and vaccine-induced immunity, Int. J. Res. Interdiscip. Stud. 1 (2023), 5–14.

[32] W. Anggraeni, M. Firdausiah, M.I. Perdana, Forecasting the case number of infectious diseases using type-2 fuzzy logic for a diphtheria case study, Eng. Proc. 39 (2023), 3. https://doi.org/10.3390/engproc2023039003.

[33] J.K. Hale, S.M.V. Lunel, Introduction to functional differential equations, Springer, New York, 2013. https://doi.org/10.1007/978-1-4612-4342-7.

[34] M. Mahrouf, K. Hattaf, N. Yousfi, Dynamics of a stochastic viral infection model with immune response, Math. Model. Nat. Phenom. 12 (2017), 15–32. https://doi.org/10.1051/mmnp/201712502.

[35] K. Hattaf, M. Mahrouf, J. Adnani, N. Yousfi, Qualitative analysis of a stochastic epidemic model with specific functional response and temporary immunity, Physica A: Stat. Mech. Appl. 490 (2018), 591–600. https://doi.org/10.1016/j.physa.2017.08.043.

[36] N. Dalal, D. Greenhalgh, X. Mao, A stochastic model of aids and condom use, J. Math. Anal. Appl. 325 (2007), 36–53. https://doi.org/10.1016/j.jmaa.2006.01.055.

[37] X. Mao, Stochastic differential equations and applications, Elsevier, 2007.

[38] O. Diekmann, J.A.P. Heesterbeek, J.A.J. Metz, On the definition and the computation of the basic reproduction ratio r 0 in models for infectious diseases in heterogeneous populations, J. Math. Biol. 28 (1990), 365–382. https://doi.org/10.1007/BF00178324.

[39] P. Van Den Driessche, J. Watmough, Reproduction numbers and sub-threshold endemic equilibria for compartmental models of disease transmission, Math. Biosci. 180 (2002), 29–48. https://doi.org/10.1016/S0025-5564(02)00108-6.

[40] A. Gray, D. Greenhalgh, L. Hu, et al. A stochastic differential equation sis epidemic model, SIAM J. Appl. Math. 71 (2011), 876–902. https://doi.org/10.1137/10081856X.

[41] World Health Organization, Diphtheria - Guinea, 2023. https://www.who.int/emergencies/disease-outbreak-news/item/2023-DON492.

[42] M.V. Murhekar, Resurgence of diphtheria in India, J. Infect. 80 (2020), 232–254. https://doi.org/10.1016/j.jinf.2019.10.010.

[43] K. Sornbundit, W. Triampo, C. Modchang, Mathematical modeling of diphtheria transmission in Thailand, Comput. Biol. Med. 87 (2017), 162–168. https://doi.org/10.1016/j.compbiomed.2017.05.031.

[44] S. Akarsu, F. Polat, Possible cutaneous adverse effects of anti-infective vaccinations, in: M.I. Choudhary (Ed.), Frontiers in Anti-Infective Drug Discovery, Bentham Science Publishers, 2024: pp. 116–149. https://doi.org/10.2174/9781681089348124100006.

[45] E. Arguni, M.R. Karyanti, H.I. Satari, et al. Diphtheria outbreak in Jakarta and Tangerang, Indonesia: epidemiological and clinical predictor factors for death, PLOS ONE 16 (2021), e0246301. https://doi.org/10.1371/journal.pone.0246301.